Local Stability and Dynamics of Apocytochrome b 562 Examined by the Dependence of Hydrogen Exchange on Hydrostatic Pressure † , ‡

ARTICLE *in* BIOCHEMISTRY · JULY 1998

Impact Factor: 3.02 · DOI: 10.1021/bi980894o · Source: PubMed

2 AUTHORS:

Ernesto J Fuentes
University of Iowa
27 PUBLICATIONS **870** CITATIONS
SEE PROFILE

Andrew Joshua Wand
University of Pennsylvania
193 PUBLICATIONS **8,748** CITATIONS
SEE PROFILE

Local Stability and Dynamics of Apocytochrome b_{562} Examined by the Dependence of Hydrogen Exchange on Hydrostatic Pressure[†,‡]

Ernesto J. Fuentes[§] and A. Joshua Wand*[,§]

Departments of Chemistry and Biological Sciences and Center for Structural Biology, State University of New York at Buffalo, Buffalo, New York 14260-3000

Received April 20, 1998; Revised Manuscript Received June 4, 1998

ABSTRACT: Hydrostatic pressure is used to perturb the manifold of states available to apocytochrome b_{562} and to examine the energetics and dynamics of the protein using hydrogen exchange monitored in real-time by heteronuclear spectroscopy at pressures ranging up to 1.1 kbar. An analytical framework for interpreting the effects of hydrostatic pressure on the physical events leading to protein hydrogen exchange is presented. The protein is found to have three regions of subglobal cooperative stability. The most stable region, or core, is composed of the central two helices of the bundle. The dependence of the global unfolding free energy upon pressure is first order and associated with a negative volume change of -102 mL mol^{-1}. Two additional regions of cooperative structure are identified, and both also have negative volume changes associated with their unfolding at high pressure. Surprisingly, one of the subglobal unfolding units shows a significant positive volume change at low pressures (<200 bar) suggesting the presence of a highly mispacked open state at ambient pressure. The three regions of cooperative stability are the same as identified by perturbation with chemical denaturant. The implications of these results for issues in protein folding and the form of the energy landscape of globular proteins are discussed.

Characterization of the origins of the cooperative nature of protein structure remains an area of intense interest and debate (*1*−*3*). The principles delineating regions of cooperatively stabilized structure within proteins are particularly important in the context of protein folding, protein design and engineering, and protein stability in general. Insight into the free energy relationships underlying fundamental units of protein structure can now be gained by a variety of approaches. A particularly appealing method relies upon the fact that, under native-like conditions, a small fraction of protein molecules will occupy higher energy, partially unfolded states as dictated by the Boltzman distribution. These states can be probed by hydrogen-exchange methods, and structural correlations can be often deduced from the response of the distribution of states to chemical denaturants or temperature (*4*−*6*). These kinds of studies often ameliorate many of the obvious difficulties and ambiguities of working with stable, equilibrium intermediates of proteins prepared under extreme solvent conditions.

Application of hydrostatic pressure generally results in the reversible unfolding of proteins in water because the volume of the protein−solvent system is smaller for the unfolded state. The potential microscopic origins of this negative volume change are numerous and include reduction in volume arising from hydrophobic solvation and electrostriction in the unfolded state and elimination of voids or packing defects in the folded state (*7*). Nevertheless, it has been pointed out that the apparent response of protein molecules to hydrostatic pressure is somewhat inconsistent with the view that formation of a hydrophobic core stabilizes globular proteins (*8*).

Here, we are interested in using hydrostatic pressure to manipulate the relative free energies of cooperative units of structure within apocytochrome b_{562}. The apoprotein retains much of the classical four-helix bundle topology of the holoprotein and displays physical features commonly associated with so-called protein "molten globules". Rather than repack its core in response to the absence of the heme prosthetic group, the apoprotein maintains a large cavern that is highly exposed to solvent (*9*). This structural feature explains many of the peculiar physical properties of the protein (*9*) such as its relatively low ΔC_p for unfolding (*10*, *11*) and its relatively low stability to chemical and thermal denaturation (*10*, *11*). The stability and dynamics of apocytochrome b_{562} have been probed by examination of the dependence of its hydrogen exchange behavior upon the presence of chemical denaturant, and the protein was found to have three regions of subglobal cooperative stability (*11*). The most stable region, or core, is composed of the central two helices of the bundle and coincides with the global stability of the molecule as seen by calorimetry and optical melts. The N- and C-terminal helices were found to be of lower stability, each comprising a subglobal folding unit.

[†] Supported by Grant GM 35940 from the National Institutes of Health and Grants DAAH04-96-1-0312 and DAAG55-97-10181 from the Army Research Office awarded to A.J.W.

[‡] Dedicated to the memory of Gregorio Weber.

* To whom correspondence should be addressed.

[§] Present address: Department of Biochemistry and Biophysics, School of Medicine, University of Pennsylvania, Philadelphia, PA 19104.

[1] Abbreviations: GdmCl, guanidinium hydrochloride; NMR, nuclear magnetic resonance; HSQC, heteronuclear single-quantum correlation; HX, hydrogen exchange; pH*, observed pH meter reading uncorrected for the isotope effect; ΔG_{HX}, free energy for global unfolding obtained from hydrogen exchange; *P*, hydrogen exchange protection factor.

S0006-2960(98)00894-0 CCC: $15.00
Published on Web 06/25/1998

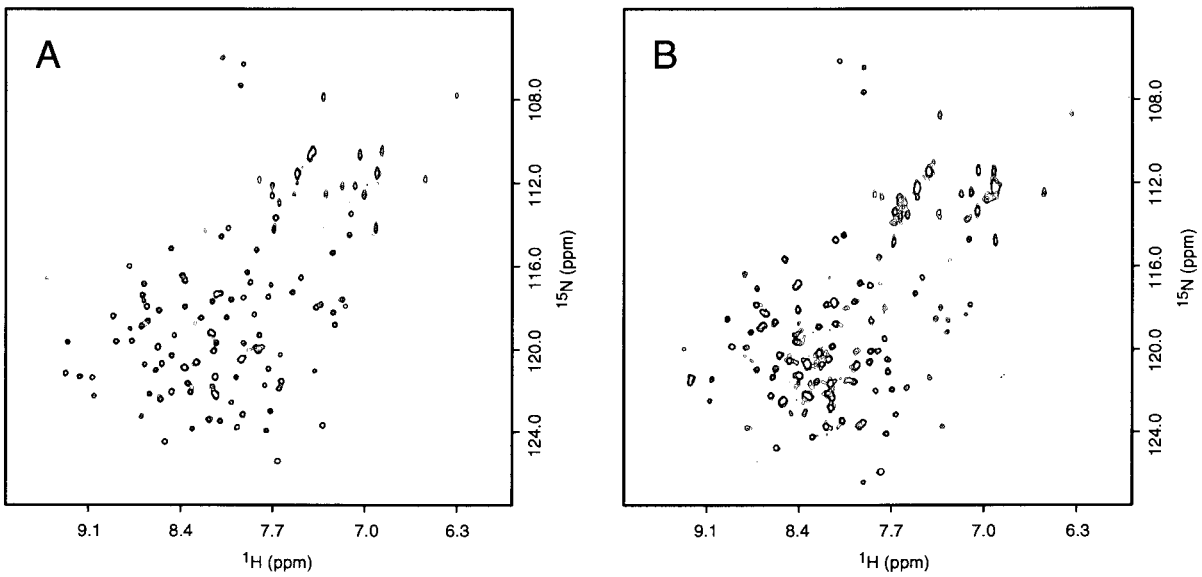

FIGURE 1: Sensitivity of the ^{15}N-HSQC spectrum of apocytochrome b_{562} to hydrostatic pressure. Shown are ^{15}N-HSQC spectra at 1 bar (A) and 1.1 kbar (B) obtained at 600 MHz (^{1}H) under conditions similar to HX experiments: 50 mM acetate buffer, pH* 4.5 in 90% D_2O, and 27 °C.

In the present study, we use pressure to perturb the manifold of states available to apocytochrome b_{562} and, for the first time, examine the energetics and dynamics of a protein using hydrogen exchange monitored in real-time by heteronuclear spectroscopy at pressures ranging up to and over 1 kbar. An analytical framework is developed to interpret the range of effects of hydrostatic pressure on the physical events leading to protein hydrogen exchange that are observed. Three regions of cooperative stability are identified and are the same as those revealed by perturbation with chemical denaturant. These and other findings have significant implications for our understanding of the energy landscape of this protein.

MATERIALS AND METHODS

Cytochrome b_{562} was obtained using a previously described T7-based expression system and purification protocol (*11*). Each NMR sample (~300 mL) contained ~2−3 mM apocytochrome b_{562} in 50 mM sodium d_3-acetate 90% D_2O/10% H_2O, pH* 4.5. Samples were prepared from a stock of protein hydrated with buffer prepared in H_2O. The hydrated sample was centrifuged to remove insoluble particulate matter. The hydrogen exchange reaction was initiated by addition of ~270 μL of buffer prepared in D_2O to ~30 μL of H_2O buffer containing 20−25 mg of protein. The residual H_2O content of the sample was on the order of ~10−15%. The dead-time of the experiment, defined as the time from the addition of D_2O buffer to initiation of the NMR experiment, was ~30 min. The desired hydrostatic pressure was reached within ~15 min of addition of D_2O buffer. The pH of the sample was determined at atmospheric pressure after the completion of the HX experiment using a conventional micro glass electrode. The pH of each sample was corrected for pressure ionization effects on the buffer as described previously (*12*). At 1.1 kbar, this correction amounts to ~0.20 pH units. The range of corrected pHs over all experiments was 4.39−4.77.

Hydrogen exchange rates were determined using serial two-dimensional sensitivity-enhanced gradient-selected ^{1}H-^{15}N HSQC spectra (*13*) using a Varian Unity-INOVA spectrometer operating at 600 MHz for ^{1}H. The spectra were collected as 64 complex points in the incremented ^{15}N time domain (t_1) and 1024 complex points in the acquisition time domain (t_2). The length of each experiment was approximately 30 or 60 min (16 or 32 scans/free induction decay, respectively). Sequential ^{1}H-^{15}N-HSQC spectra were collected up to 3000 min, as required. Spectra were processed using Felix (Biosym Technologies Inc.) and hydrogen exchange rates extracted as described previously (*11*).

High-pressure NMR was performed using an apparatus which employs a high-pressure cell technique allowing state-of-the-art NMR spectroscopy at kilobar pressures without modification of the spectrometer (Ehrhardt et al., in preparation; *14*). We have employed a sapphire tube fitted to a BeCu charging valve and have used liquid pressurization to increase the reliability and safety of the device. Pressurization was achieved using ethanol as pressurization liquid and a hand-driven pump system. The nominal volume of the sample was ~100 μL. The sample was isolated from the water used to transmit the pressure by use of mineral oil (Sigma).

RESULTS

Native State Hydrogen Exchange. Using serial ^{1}H-^{15}N-HSQC NMR spectroscopy, hydrogen exchange rates for 54 of 102 amide protons in apocytochrome b_{562} could be measured at pH* 4.5 and 27 °C at hydrostatic pressures ranging up to 1.1 kbar. Hydrogen exchange rates greater than ~2−3 h^{-1} could not be determined using this real-time NMR spectroscopic method. The effect of hydrostatic pressure on the NMR spectrum of apocytochrome b_{562} is minor at all pressures used in this study (Figure 1).

A total of 15 hydrogen exchange experiments were conducted at eight pressures ranging from ambient pressure to 1.1 kbar. Replicate measurements at 1 bar (×2), 75 bar (×2), 150 bar (×3), and 500 bar (×3) allowed for an estimation of the precision of the obtained rates. The precision of obtained rate constants estimated from analysis of residuals to the fits averaged 2.5% relative error over all

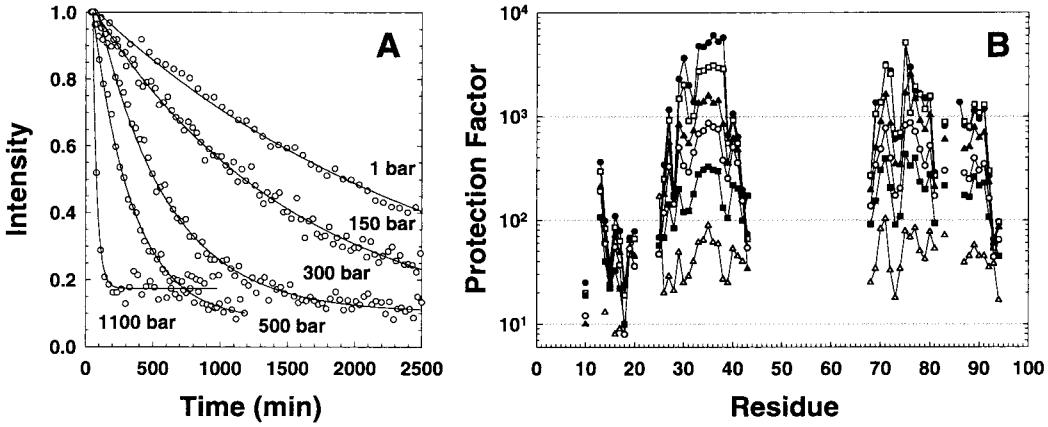

FIGURE 2: Summary of hydrogen exchange data obtained. Representative amide hydrogen exchange curves for Ala-37 are shown in panel A. Intensities are normalized to the initial intensity. Amides with faster exchange rates have smaller initial absolute intensities and therefore different ending relative intensities. Protection factors for apocytochrome b_{562} obtained at six of the eight hydrostatic pressures examined are shown in panel B [~1 bar (●), 150 bar (□), 300 bar (▲), 500 bar (○), 700 bar (■), 1.1 kbar (△)].

data. Independent replicates of hydrogen exchange data sets gave an average variance in the obtained apparent free energy of 0.22 kcal mol^{-1} (see eq 2). Examples of hydrogen exchange curves obtained as a function of pressure are shown in Figure 2 for the amide of Ala-37, and serve to illustrate the quality of data obtained in this study. The effective dead-time for the experiments was approximately 30 min and the obtained rates span 0.022−1.8 h^{-1}.

Assuming that the rate of closing (k_{cl}) from the hydrogen exchange competent state(s) to the hydrogen bonded, exchange incompetent state is much faster than the rate of chemical catalysis, the so-called EX2 condition prevails, and the effective equilibrium opening constant (K_{op}) can be obtained from the observed rate of exchange (k_{obs}) and knowledge of the underlying chemical rate (k_{chem}) (*15*, *16*).

$$k_{obs} = \frac{k_{op}}{k_{op} + k_{cl}} k_{chem} \approx \frac{k_{op}}{k_{cl}} = K_{op} k_{chem} \qquad (1)$$

The EX2 limit provides access to the free energy of opening via eq 2.

$$\Delta G_{HX}^{eff} = -RT \ln K_{op} \qquad (2)$$

Although the basic chemistry of hydrogen exchange virtually guarantees the EX2 limit at atmospheric pressure under the solution conditions used here (pH* 4.5, 27 °C), it has been shown that high pressure may significantly slow the rate of folding relative to that of unfolding (*17*). Thus, the dominance of the EX2 limit at high pressures requires confirmation. A direct test of the EX2 condition is to vary the pH at which exchange is carried out and confirm that the change in the observed hydrogen exchange rate is as predicted by the corresponding change in k_{chem} (*6*). Such a test was carried out under the highest pressure employed (1.1 kbar). Logarithms of hydrogen exchange rates obtained at pH* 4.39 and 4.82 (pressure corrected) showed a linear correlation (slope ~0.9) with correlation coefficient of 0.98, thus reinforcing the expectation that the EX2 condition is present.

Hydrogen Exchange Catalysis. The definition of random coil exchange rates, k_{chem}, is now routinely determined by use of empirical calibrations for sequence specific, solution, and temperature effects upon the chemistry of hydrogen exchange (*18*, *19*). At high pressures, however, one also needs to account for the effects of pressure. Here, we calculate k_{chem} for each exchangeable backbone amide hydrogen, taking into account nearest neighbor and inductive effects (*18*) and isotope content (*20*) as a function of temperature (*19*) and pressure (*21*, *22*). Temperature effects on acid, base, and water exchange rate constants were corrected using eq 3.

$$k(T) = k_0(T_0) \exp\left[-\frac{E_a}{R}\left(\frac{1}{T} - \frac{1}{T_0}\right)\right] \qquad (3)$$

where k_0 is the reference random coil exchange rate constant determined at T_0 (293 K), the reference temperature. The activation energies recommended by Bai et al. (*18*) were used: 14, 3, and 19 kcal mol^{-1} for $E_a(H^+)$, $E_a(OH^-)$, and $E_a(H_2O)$, respectively.

Following the principle of Le Chatelier, an increase in pressure on a system will cause a shift of the equilibrium toward the state where the system volume is minimized. Similarly, the pressure dependence of a kinetic process is described by eq 4 for a discrete pressure change, where the reference rate constant and presssure are k_0 and p_0 (1 bar), respectively.

$$k(p) = k_0(p_0) \exp\left[-\frac{(p - p_0)}{RT} \Delta V^{\dagger}\right] \qquad (4)$$

The acid, base, and water hydrogen exchange rate constants were corrected for pressure effects using eq 4 and the following activation volumes: $\Delta V^{\dagger}_{H^+} = +1.7$ mL mol^{-1}, $\Delta V^{\dagger}_{OH^-} = +11$ mL mol^{-1}, $\Delta V^{\dagger}_{H_2O} = -9$ mL mol^{-1} (*23*).

The ionization constant of water, K_w, is both temperature and pressure dependent. The temperature dependence of the ionization constant of D_2O has been determined by Covington et al. (*24*) and the pressure dependence has been addressed by Hamann (*25*) and Millero et al. (*26*). The dependence of K_w (D_2O) on pressure was estimated using eq 5. The constant b has been empirically determined to be 9.2×10^{-5} bar^{-1} (*25*, *27*).

$$pK_W(T, p) - pK_W(T, p_0) = -\frac{p\Delta V_{K_w}}{2.303RT(1 + bp)} \qquad (5)$$

An ionization volume of water (ΔV_{K_w}) of -22.1 mL mol^{-1} was used (*28*).

The ionization state of acidic side chains was estimated by using the pK_a of the free amino acid correcting for temperature and pressure effects as described above. The ionization volume for the side chain carboxylic acid (ΔV_{K_a}) was taken as -11.4 mL mol^{-1} (*12*). The effect of pressure on the pK_a of the buffer was similarly corrected. The value of the activation energy for Glu and Asp side-chain carboxyl was taken as 1083 and 1000 cal mol^{-1}, respectively. It should be noted that, despite the relative complexity of the corrections required, the overall change in k_{chem} over the pressure range used is small, usually on the order of 1.5−2-fold.

Determination of Effective Equilibrium Opening Constants (K_{HX}^{eff}). Given k_{chem}, the effective equilibrium opening constant defined by eq 1 or its inverse, the protection factor (P) can be determined. Figure 2 shows the protection factors plotted as a function of residue number obtained at several pressures. The range of determined protection factors spans approximately 2 orders of magnitude reaching a maximum of 10^4 and a minimum of approximately 20, the lower limit of reliable quantification. At ambient pressure, four distinct regions of protection are evident, each encompassing a region known to be helical in the solution structure of the apoprotein (*9*). These and other features of the hydrogen exchange behavior of the protein under ambient pressure conditions have been discussed in detail previously (*11*).

Analysis of the Mechanisms of Hydrogen Exchange. The physical origin of the "opening" events that lead to productive exchange of amide hydrogens with solvent is of central interest here. Our analysis begins with the framework of Englander and co-workers which describes the observed, effective equilibrium opening constant as a sum of three physically distinct processes (for a review, see ref *29*).

$$K_{HX}^{eff} = K_{HX}^{local} + K_{HX}^{subglobal} + K_{HX}^{global} \quad (6)$$

Here, physical events arising from local, larger but subglobal, and global unfolding motions can each lead to productive exposure of an amide hydrogen to solvent. In the absence of additional information, it is difficult to deconvolve the various contributions to K_{HX}^{eff}. However, Bai et al. (*30*) have noted that local, subglobal, and global unfolding events are likely to respond differently to the effects of chemical denaturant and temperature. Thus, perturbation of hydrogen exchange behavior in proteins as a function of chemical denaturant concentration or temperature may not only allow determination of the origin of K_{HX}^{eff} but can also identify regions of subglobal cooperativity in proteins. There are now several examples of the use of chemical denaturants or temperature to promote hydrogen exchange in proteins (*4*, *11*, *30*−*32*). In the case of chemical denaturants, the acceleration of hydrogen exchange is related to the stabilization of the exchange competent state(s) relative to the native (exchange incompetent state) via binding to the increased accessible surface area.

Pressure Dependence of the Equilibrium Leading to Hydrogen Exchange. The relationship between the perturbation of the free energy change (dΔG) associated with each of the individual equilibrium constants of eq 6 and pressure can be expressed as

$$d\Delta G = \Delta G(p_1) - \Delta G(p_0) \quad (7)$$

where p_0 and p_1 are the beginning and ending pressures, respectively. The dependence of the change in free energy of a system at p_1 can be generally expressed in terms of its free energy at p_0 by

$$\Delta G(p_1) = \Delta G(p_0) + \int_{p_0}^{p_1} \Delta V \, dp \quad (8)$$

In the absence of an explicit functional form for the pressure dependence of the change in system volume (ΔV), eq 8 can be solved by a Taylor series expansion about the reference pressure, p_0 (*33*). For small ($p_1 - p_0$), we have

$$\Delta G(p_1) = \Delta G^\circ + (\Delta V^\circ)(p_1 - p_0) + \frac{1}{2}\left(\frac{d\Delta V^\circ}{dp}\right) \times (p_1 - p_0)^2 + \frac{1}{6}\left(\frac{d^2\Delta V^\circ}{dp^2}\right)(p_1 - p_0)^3 \quad (9)$$

where the degree symbol refers to the reference state at p_0, and we note that the difference in isothermal compressibility between the two states ($\Delta\kappa$) is defined as $(-\partial\Delta V/\partial p)_T$. Clearly, the dependence of ΔG on pressure can potentially be quite complicated. The sign of the quadratic term can be positive or negative, depending on whether the application of pressure drives the reaction forward or backward. The cubic term effectively contains the pressure dependence of $\Delta\kappa$, which can, in principle, also be either positive or negative. When $\Delta\kappa$ and $d\Delta\kappa/dp$ are small, the volume change is independent of pressure and eq 9 reduces to the usual first-order dependence of ΔG on pressure:

$$\Delta G(p_1) = \Delta G^\circ + \Delta V^\circ(p_1 - p_0) \quad (10)$$

Equations 9 and 10 allow us to explore the form of hydrogen exchange curves as a function of the system parameters: ΔG°, ΔV°, and $\Delta\kappa$. Recasting eq 6 in terms of eq 9 gives a general relationship for the dependence of hydrogen exchange of a given amide hydrogen on pressure, which is significantly more complicated than its counterpart describing the dependence of ΔG_{HX}^{eff} on chemical denaturant (see eq 6 of ref *11*). Nevertheless, there are some clear graphical limits. For example, a linear dependence of the change in free energy (ΔG_{HX}) throughout a given pressure range corresponds to the case described by eq 10 and indicates the dominance of a single equilibrium having a negligible change in isothermal compressibility with pressure. An increase in the change of free energy at low pressure suggests a positive ΔV°, and so on.

Identification of Cooperative Units. A central goal of this effort is to identify units of subglobal cooperative stability in the protein by using pressure as a correlating perturbation. We will follow closely the treatment presented earlier for an analogous study of the effects of chemical denaturant (*11*). Ideally, the first step in this analysis is to identify those amide hydrogens whose exchange is dominated by the contribution of global unfolding at high pressure and little or no significant local or subglobal contributions. Identifying these amides amounts to finding those which show the same dependence of ΔG_{HX}^{eff} with pressure associated with the largest negative ΔV°. The amides of residues 34−37 and 75−77 share a

common $\Delta V°$ value of -102 ± 3 mL mol^{-1} which was the most negative found. Residues 34−37 and 76 have a strictly linear dependence while residues 75 and 77 show a slightly nonlinear behavior at low pressures (Figure 3, panel A). The linearity indicates that eq 10 applies and the associated volume change can be taken directly from the slope of the line. The fitted associated global free energy, ΔG_{HX}, was found to be 5.17 ± 0.05 kcal mol^{-1}. When corrected for proline isomerization (*6*), the free energy becomes ∼4.8 kcal mol^{-1}, which is consistent with previous results for global unfolding (*11*). It is very important to note that the residues associated with global unfolding found here are essentially the same as those found by perturbation of the hydrogen exchange behavior with GdmCl (*11*).

A similar search was carried out for additional sets of hydrogens which share a common subglobal parameter set with the contribution from global unfolding included. The core of one such group involves residues 87−91 in helix IV and has associated ΔG_{HX} (uncorrected) and $\Delta V°$ parameters of 4.56 ± 0.26 kcal mol^{-1} and -65 ± 5 mL mol^{-1}, respectively. Again, the amides found to define this cooperative unit are the same as those found by hydrogen exchange with GdmCl (*11*). It is interesting to note that this group of amides shows a distinct rise in the free energy associated with exchange over low pressures which is rapidly overcome by a linear decrease in the free-energy associated with exchange at higher pressures (Figure 3, panel B). This is the only region of the protein where this type of behavior is seen. As *all* of these amides show effectively the same pattern of response to pressure, one is led to conclude that it is a property of a subglobal event rather than a contribution from exchange via a local unfolding event.

A subglobal cooperative unit of structure is also potentially located in helix I. Though the protection factors are derived from hydrogen exchange rates at the limit of our detection, residues 15−17, 19, and 20 appear to form a cooperative unit as indicated by the convergence of the individual ΔG_{HX}^{eff} (p) curves to a common isotherm at high pressure (Figure 3, panel C). The linear region of these curves at low pressures indicate apparent ΔG_{HX} values ranging from 3.58 ± 0.24 (for N13) to 2.01 ± 0.22 (for K15) kcal mol^{-1} and apparent $\Delta V°$ values ranging from -41 ± 14 (for N13) to -7 ± 11 (for K15) mL mol^{-1}. There is no hint of a positive inflection at low pressures, as seen for the residues in helix IV. At higher pressures (>∼1 kbar), all curves show a definite downward curvature. This type of behavior would be consistent either with locally dominated exchange at low pressures being overtaken by subglobal exchange at higher pressures or with pressure-dependent subglobal exchange dominating throughout. The data are insufficient to distinguish between the two possbilities.

DISCUSSION

Apocytochrome b_{562} is an example of a protein whose folding (and stability) is frustrated by the absence of an integral component of the final, native structure—a heme prosthetic group. In contrast to many models of metastable states of proteins generated by extreme conditions (such as low pH), apocytochrome b_{562} may be studied under near native conditions, which is directly applicable to the question of the folding and assembly of the protein into its final holo form. Recently, the range of local stabilities and cooperative structural units within apocytochrome b_{562} were explored using native-state hydrogen exchange as a function of chemical denaturant concentration (*11*). Three regions of cooperative structure were indicated with the two central helices of the bundle forming the core of the protein and the N- and C-terminal helices each forming independent cooperative units of lower stability. The present study was very much motivated by a desire to determine whether structural perturbation by pressure reveals the same cooperative units of structure as revealed by chemical denaturant.

The possibility that proteins may have fundamental units of cooperativity, or building blocks, has received significant attention in the recent literature (*3*, *30*). Bai et al. (*29*, *30*) have illustrated how the binding of chemical denaturants or a change in temperature can redistribute the protein ensemble and thereby allow the correlation of otherwise apparently uncorrelated amide hydrogen exchange. The astonishing result was that despite the means by which the ensemble was perturbed (denaturant or temperature), a direct correspondence of cooperative units was found. This result poses an interesting question: are cooperative units of protein structure unique and so far removed from other possible states in free energy that virtually any simple perturbation will reveal the same set? The answer to this question has enormous implications in protein folding, the form of the energy landscape of a globular protein, etc., and could ultimately have a tremendous impact on the emerging field of protein design. Here, the answer appears to be yes.

Character of Cooperative Units of Structure. The global stability of apocytchrome b_{562} has been previously investigated by calorimetry, GdmCl denaturation, and native-state hydrogen exchange using GdmCl (*11*). Native-state hydrogen exchange analysis of residues clustered in the two central helices (32−37, 70, 72, and 75−77) were found to have similar free energies and dependence on GdmCl (m value) as determined by calorimetry and GdmCl denaturation, indicating that the behavior of these residues is indeed representative of global unfolding. In the present study, the use of pressure to perturb the hydrogen exchange behavior of the protein also identifies the two central helices as the most stable region of the molecule. The unfolding associated with hydrogen exchange in this region of the molecule is associated with a ΔG_{HX} ∼5.2 kcal mol^{-1} and a $\Delta V° \sim -102$ mL mol^{-1}. This free energy change is comparable to that found previously using calorimetry and native-state hydrogen exchange with GdmCl (*11*).

The identification of a negative and essentially constant volume change associated with the global unfolding of the protein over pressures ranging from ambient pressure to 1.1 kbar is in itself surprising. Sometime ago, Kauzman pointed out that the simple liquid hydrocarbon model, upon which the hydrophobic effect is commonly modeled, fails to predict the observed pressure dependence of protein denaturation: the volume change for the transfer of hydrocarbons into water is negative at low pressure and positive at high pressures (*8*). Model studies of hydrophobic solvation (*34*) indicate that the observed ΔV will become positive in the 1−2 kbar pressure region. There is some confusion in the recent literature about the precise nature of the apparent paradox (*35*−*37*). It appears that at low pressures, the earlier experimental results for proteins of a small negative change

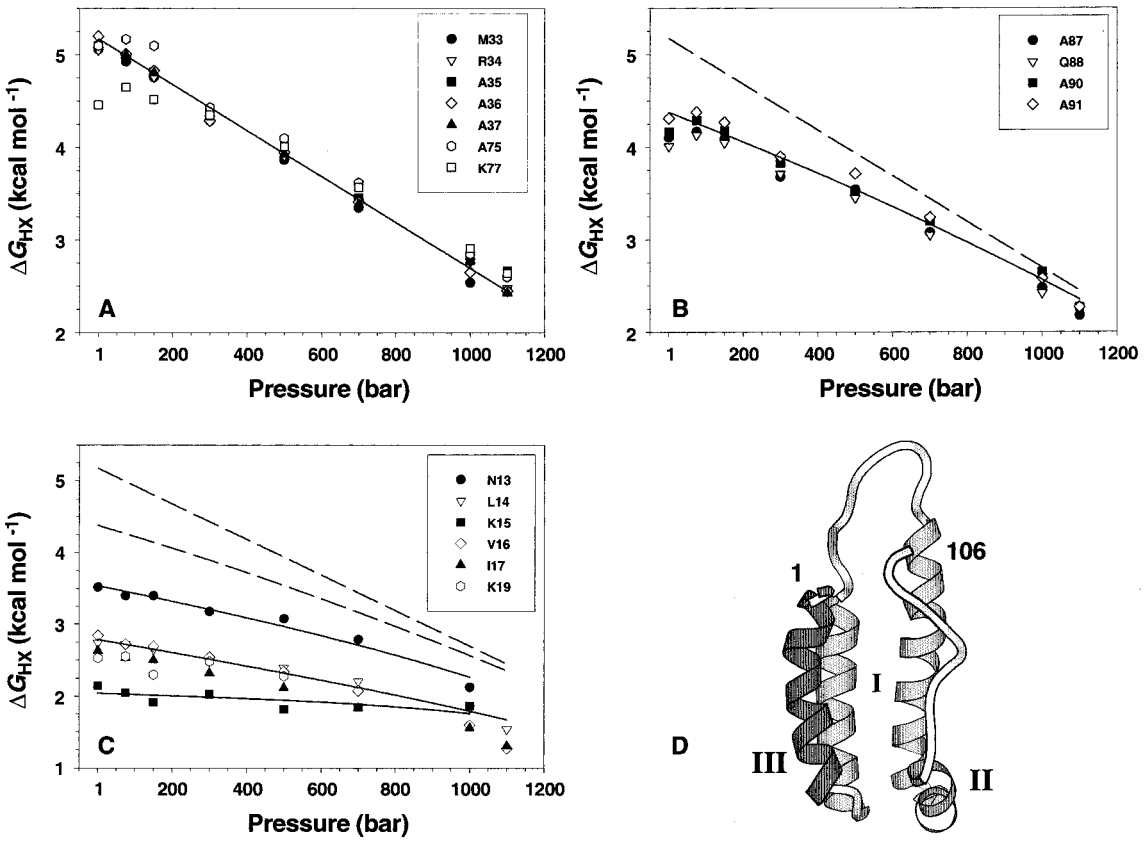

FIGURE 3: Segregation of individual amides into cooperative units on the basis of the dependence of ΔG_{HX}^{eff} on hydrostatic pressure. Panel A shows the ΔG_{HX}^{eff} of residues 34−37 and 75−77 of cooperative unit I as a function of pressure. The solid line corresponds to eq 10 using the $\Delta G°$ and $\Delta V°$ values obtained. Panel B shows a similar plot for residues 87−92 of cooperative unit II. The solid line corresponds to eq 10 using the $\Delta G°$ and $\Delta V°$ values obtained and includes the global contribution. The dashed line corresponds to the global isotherm. Panel C shows the ΔG_{HX}^{eff} of residues 13−19 of cooperative unit III as a function of pressure. The solid lines corresponds to eq 10 using the $\Delta G°$ and $\Delta V°$ values obtained for N13, L14, and K15 in the low-pressure range. The downward deflection at high pressures is attributable to the contribution from global unfolding. The dashed lines correspond to the isotherms of the other cooperative units. In all cases the ΔG_{HX} values shown are uncorrected for the proline effect (see text). Panel D shows a ribbon representation (*43*) of the solution structure of apocytochrome b_{562} (*9*).

in volume (∼−50 to −100 mL mol^{-1}) was considered too positive while the predicted positive change in volume at higher pressures was not observed at all.[2] This apparent paradox has been recently rationalized from several different perspectives (*33*, *38*−*40*). In the case of apocytochrome b_{562} the volume change associated with global unfolding is clearly negative at low pressures (<1 kbar) and shows no sign of the nonlinearity predicted by the hydrocarbon model at higher pressures (*34*). This seems to suggest that the difference in isothermal compressibility between the folded and unfolded states is very small. This is consistent with the fact that the folded state of apocytochrome b_{562} has an unusually large exposed hydrophobic surface.

In addition to the global opening, two distinct subglobal openings are also detected. Significantly, they also correspond to the same cooperative units found by using GdmCl as a perturbant of hydrogen exchange (*11*). Specifically, residues in helix I having ΔG_{HX} values ranging between ∼3.6 and ∼2.0 kcal mol^{-1} and apparent $\Delta V°$ values ranging between ∼−41 and −7 mL mol^{-1} correspond to a cooperative unit identified by chemical denaturant hydrogen exchange. Similarly, residues in helix IV that are associated with a $\Delta G_{HX} \sim 4.6$ kcal mol^{-1} and a $\Delta V° \sim -65$ mL correspond to a cooperative unit also identified by chemical denaturant hydrogen exchange (*11*). The $\Delta V°$s obtained are only loosely correlated with the corresponding *m* values which is not entirely surprising (*42*).

The Local Dynamics of Apocytochrome b_{562}. The ΔG_{HX}^{eff} of most of the amide NH associated with the cooperative units of structure identified have a downward concave or linear dependence with pressure at relatively low pressures (<200 bar) (Figure 3). Linearity corresponds to the domination of a single term in eq 6, i.e., a single type of opening which has little second-order dependence upon pressure. A flat response of an amide hydrogen ΔG_{HX}^{eff} to this low pressure range which is subsequently followed by a linear response at higher pressures suggests a small local $\Delta V°$. A more interesting result is the occurrence of a definite increase in ΔG_{HX}^{eff} with pressure at relatively low pressures. This is seen uniquely for the residues in helix IV (Figure 3, panel B). As all residues that define this cooperative unit display this feature, it must be a characteristic of the subglobal unfolding event. Furthermore, the upward inflection at low pressure must be due to a significant and positive $\Delta V°$. Since the electrostriction and hydrophobic solvation that accompanies unfolding is generally thought to lower the system

[2] Recently, Markley and co-workers (*41*) have determined a small but significant difference in the isothermal compressibility of the folded and unfolded states of ribonuclease A, which would lead to a positive ΔV at high pressures.

volume, the apparent increase in volume observed for this subglobal unfolding implies that the corresponding partially unfolded state is much more poorly packed than the folded state. It is also rapidly destabilized as the pressure passes ~150 bar, resulting in the presumably more relaxed (efficiently solvated) partially unfolded state associated with higher pressures dominating the hydrogen exchange detected manifold of states.

Conclusions. A method has been introduced which employs perturbation of hydrogen exchange behavior of proteins by hydrostatic pressure to allow the identification of regions of subglobal structural cooperativity. The information complements the view provided by perturbation with chemical denaturant and, in the case of apocytochrome b_{562}, identifies the same regions of structural cooperativity. This suggests that the free energy landscape available to this protein is marked by the dominance of three conformational states. The absence of a significant pressure dependence on the apparent change in system volume connecting these three states indicates that the folded and unfolded states of this protein have closely similar isothermal compressibilities. Different regions of the protein display different sensitivity to pressure at relatively low pressures, indicating that the local and subglobal unfolded states can have a range of packing efficiencies.

ACKNOWLEDGMENT

We are grateful to Drs. Peter Flynn, Mark Ehrhardt and Andrew Lee for assistance with the NMR spectroscopy at high pressure and Professor John Markley for sharing results prior to publication.

REFERENCES

1. Lesk, A. M., and Rose, G. D. (1981) *Proc. Natl. Acad. Sci. U.S.A. 78*, 4304−8.
2. Murphy, K. P., Bhakuni, V., Xie, D., and Freire, E. (1992) *J. Mol. Biol. 227*, 293−306.
3. Panchenko, A. R., Luthey-Schulten, Z., Cole, R., and Wolynes, P. G. (1997) *J. Mol. Biol. 272*, 95−105.
4. Mayo, S. L., and Baldwin, R. L. (1993) *Science 262*, 873−6.
5. Kim, K. S., Fuchs, J. A., and Woodward, C. K. (1993) *Biochemistry 32*, 9600−8.
6. Bai, Y., Milne, J. S., Mayne, L., and Englander, S. W. (1994) *Proteins 20*, 4−14.
7. Weber, G., and Drickamer, H. G. (1983) *Q. Rev. Biophys. 16*, 89−112.
8. Kauzmann, W. (1987) *Nature 325*, 763−4.
9. Feng, Y., Sligar, S. G., and Wand, A. J. (1994) *Nat. Struct. Biol. 1*, 30−5.
10. Feng, Y., Wand, A. J., and Sligar, S. G. (1991) *Biochemistry 30*, 7711−7.
11. Fuentes, E. J., and Wand, A. J. (1998) *Biochemistry 37*, 3687−98.
12. Neuman, J., R. C., Kauzmann, W., and Zipp, A. (1973) *J. Phys. Chem. 77*, 2687−91.
13. Kay, L. E., Keifer, P., and Saarinen, T. (1992) *J. Am. Chem. Soc. 114*, 10663−65.
14. Urbauer, J. L., Ehrhardt, M. R., Bieber, R. J., Flynn, P. F., and Wand, A. J. (1996) *J. Am. Chem. Soc. 118*, 11329−30.
15. Hvidt, A., and Nielsen, S. O. (1966) *Adv. Protein Chem. 21*, 287−386.
16. Englander, S. W., and Kallenbach, N. R. (1984) *Q. Rev. Biophys. 16*, 521−655.
17. Vidugiris, G. J., Markley, J. L., and Royer, C. A. (1995) *Biochemistry 34*, 4909−12.
18. Bai, Y., Milne, J. S., Mayne, L., and Englander, S. W. (1993) *Proteins 17*, 75−86.
19. Connelly, G. P., Bai, Y., Jeng, M. F., and Englander, S. W. (1993) *Proteins 17*, 87−92.
20. Schowen, K. B. J. (1978) *Solvent hydrogen isotope effects*, Plenum Press, New York.
21. Carter, J. V., Knox, D. G., and Rosenberg, A. (1978) *J. Biol. Chem. 253*, 1947−53.
22. Nash, D. P., and Jonas, J. (1997) *Biochemistry 36*, 14375−83.
23. Mabry, S. A., Lee, B. S., Zheng, T. S., and Jonas, J. (1996) *J. Am. Chem. Soc. 118*, 8887−90.
24. Covington, A. K., Robinson, R. A., and Bates, R. G. (1966) *J. Phys. Chem. 70*, 3820−4.
25. Hamann, S. D. (1982) *J. Solution Chem. 11*, 63−8.
26. Millero, F. J., Hoff, E. V., and Kahn, L. (1972) *J. Solution Chem. 1*, 309−27.
27. El′yanov, B. S., and Hamann, S. D. (1975) *Aust. J. Chem. 28*, 945−54.
28. Dunn, L. A., Stokes, R. H., and Hepler, L. G. (1965) *J. Phys. Chem. 69*, 2808.
29. Bai, Y., and Englander, S. W. (1996) *Proteins 24*, 145−51.
30. Bai, Y., Sosnick, T. R., Mayne, L., and Englander, S. W. (1995) *Science 269*, 192−7.
31. Clarke, J., and Fersht, A. R. (1996) *Folding Des. 1*, 243−54.
32. Chamberlain, A. K., Handel, T. M., and Marqusee, S. (1996) *Nat. Struct. Biol. 3*, 782−7.
33. Payne, V. A., Matubayasi, N., Murphy, L. R., and Levy, R. M. (1997) *J. Phys. Chem. 101*, 2054−60.
34. Sawamura, S., Kitamura, K., and Taniguchi, Y. (1989) *J. Phys. Chem. 93*, 4931−5.
35. Brandts, J. F., Oliveira, R. J., and Westort, C. (1970) *Biochemistry 9*, 1038−47.
36. Hawley, S. A. (1971) *Biochemistry 10*, 2436−42.
37. Zipp, A., and Kauzmann, W. (1973) *Biochemistry 12*, 4217−28.
38. Harpaz, Y., Gerstein, M., and Chothia, C. (1994) *Structure 2*, 641−9.
39. Chalikian, T. V., and Breslauer, K. J. (1996) *Biopolymers 39*, 619−26.
40. Hummer, G., Garde, S., Garcia, A. E., Paulaitis, M. E., and Pratt, L. R. (1998) *Proc. Natl. Acad. Sci. U.S.A. 95*, 1552−5.
41. Prehoda, K. E., Mooberry, E. S., and Markley, J. L. (1998) *Biochemistry 37*, 5785−90.
42. Frye, K. J., Perman, C. S., and Royer, C. A. (1996) *Biochemistry 35*, 10234−39.
43. Kraulis, P. J. (1991) *J. Appl. Crystallogr. 24*, 946−50.

BI980894O